

Exploiting the Gate Opening Effect in a Flexible MOF for Selective Adsorption of Propyne from C1/C2/C3 Hydrocarbons

Libo Li,^a Rajamani Krishna,^b Yong Wang,^a Jiangfeng Yang,^{a,*} and Jinping Li^{a,*}

^aCollege of Chemistry and Chemical Engineering, Taiyuan University of Technology, Taiyuan 030024, Shanxi, P. R. China. Email: jpli211@hotmail.com

^bVan 't Hoff Institute for Molecular Sciences, University of Amsterdam, Science Park 904, 1098 XH Amsterdam, The Netherlands.

Contents

1. Synthetic process of [Cu(dhbc) ₂ (4,4'-bipy)].....	1
2. Fitting of experimental data on pure component isotherms.....	2
3. Molar enthalpy of gate opening.....	5
4. Isosteric heat of adsorption.....	6
5. The simulation details of Grand canonical Monte Carlo (GCMC) simulations.....	6
6. The details of MD (Molecule Dynamic) simulations.....	7
7. IAST calculations of mixture adsorption.....	8
8. Transient breakthroughs in fixed bed adsorber.....	10
9. Details of breakthrough experiment.....	12
10. C ₂ H ₂ -C ₂ H ₄ -C ₂ H ₆ separation.....	13
11. CH ₄ -C ₂ H ₆ -C ₃ H ₈ separation.....	13
12. C ₂ H ₄ -C ₃ H ₆ separation.....	13

1. Synthesis of [Cu(dhbc)₂(4,4'-bipy)]

Syntheses of [Cu(dhbc)₂(4,4'-bipy)]·H₂O were first reported by S. Kitagawa in 2003, and the synthetic processes were subsequently improved as described in our previous work. All chemicals were purchased in their highest available commercial purity (>98%) from Sigma–Aldrich.

[Cu(dhbc)₂(4,4'-bipy)]·H₂O: an ethanol solution (10 mL) containing a mixture of 4,4'-bipyridine (0.125 g, 0.8 mmol) and 2,5-dihydroxybenzoic acid (0.49 g, 3.2 mmol) was carefully layered on

the top of an aqueous solution (10 mL) of $\text{Cu}(\text{NO}_3)_2 \cdot 3\text{H}_2\text{O}$ (0.099 g, 0.4 mmol), after which green crystals began to form immediately. Three days later, the green crystals were collected by filtration, and were then washed with ethanol (Yield > 80%).

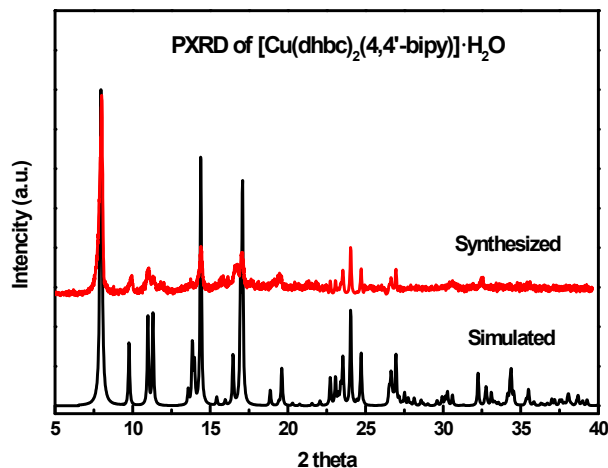


Figure S1. PXRD data for as-synthesized $[\text{Cu}(\text{dhbc})_2(4,4'\text{-bipy})] \cdot \text{H}_2\text{O}$.

2. Fitting of experimental data on pure component isotherms

The isotherm data for CH_4 were fitted with the single-site Langmuir-Freundlich model

$$q = q_{\text{sat}} \frac{bp^v}{1 + bp^v} \quad (1)$$

with T-dependent parameter

$$b = b_0 \exp\left(-\frac{E}{RT}\right) \quad (2)$$

The isotherm data for C_2H_2 , C_2H_4 , and C_2H_6 were fitted with the Dual-site Langmuir-Freundlich model, individually for each temperature

$$q = q_{A,\text{sat}} \frac{b_A p^{v_A}}{1 + b_A p^{v_A}} + q_{B,\text{sat}} \frac{b_B p^{v_B}}{1 + b_B p^{v_B}} \quad (3)$$

The pure component isotherm data for C_3H_4 , C_3H_6 and C_3H_8 display multiple inflections and a proper description of these is provided by the 3-site Langmuir-Freundlich model:

$$q = q_{A,\text{sat}} \frac{b_A p^{v_A}}{1 + b_A p^{v_A}} + q_{B,\text{sat}} \frac{b_B p^{v_B}}{1 + b_B p^{v_B}} + q_{C,\text{sat}} \frac{b_C p^{v_C}}{1 + b_C p^{v_C}} \quad (4)$$

The saturation capacities q_{sat} , Langmuir constants b , and the Freundlich exponents v , for CH_4 , C_2H_2 , C_2H_4 , and C_2H_6 , C_3H_4 , C_3H_6 and C_3H_8 are provided in supporting information.

The 1-site Langmuir-Freundlich model parameters for CH₄ are specified in Table 1. And the 2-site Langmuir-Freundlich parameters for C₂H₂, C₂H₄, and C₂H₆ are provided in Table 2, and Table 3. And the saturation capacities q_{sat} , Langmuir constants b , and the Freundlich exponents v , for C₃H₄, C₃H₆ and C₃H₈ are provided in Table 4, and Table 5.

Table 1 T-dependent Langmuir-Freundlich parameter fits for CH₄ in [Cu(dhbc)₂(4,4'-bipy)].

	q_{sat} (mol kg ⁻¹)	b_0 (Pa ⁻¹)	v (dimensionless)	E (kJ mol ⁻¹)
CH ₄	0.1	1.15×10^{-6}	0.95	8.5

Table 2 2-site Langmuir-Freundlich parameters for C₂H₂, C₂H₄, and C₂H₆ at 273 K in [Cu(dhbc)₂(4,4'-bipy)].

	Site A			Site B		
	$q_{i,A,\text{sat}}$ (mol kg ⁻¹)	$b_{i,A}$ (Pa ^{-v_i})	$v_{i,A}$ (dimensionless)	$q_{i,A,\text{sat}}$ (mol kg ⁻¹)	$b_{i,A}$ (Pa ^{-v_i})	$v_{i,A}$ (dimensionless)
C ₂ H ₂	1.4	2.35×10^{-25}	5.8	2.5	3.58×10^{-11}	2.36
C ₂ H ₄	2.7	3.25×10^{-46}	10	0.09	3.2×10^{-10}	2.55
C ₂ H ₆	2.9	1.52×10^{-28}	6.15	0.2	2.43×10^{-10}	2.1

Table 3 2-site Langmuir-Freundlich parameters for C₂H₂, C₂H₄, and C₂H₆ at 298 K in [Cu(dhbc)₂(4,4'-bipy)].

	Site A			Site B		
	$q_{i,A,\text{sat}}$ (mol kg ⁻¹)	$b_{i,A}$ (Pa ^{-v_i})	$v_{i,A}$ (dimensionless)	$q_{i,A,\text{sat}}$ (mol kg ⁻¹)	$b_{i,A}$ (Pa ^{-v_i})	$v_{i,A}$ (dimensionless)
C ₂ H ₂	3	2.82×10^{-26}	5.46	0.06	2.87×10^{-7}	1.7
C ₂ H ₄	2.35	1.82×10^{-49}	10.1	0.08	3.17×10^{-6}	1.44
C ₂ H ₆	2.6	3.49×10^{-39}	8.1	0.05	5.56×10^{-7}	1.6

Table 4 3-site Langmuir-Freundlich parameters for C₃H₄, C₃H₆ and C₃H₈ at 273 K in [Cu(dhbc)₂(4,4'-bipy)].

	C ₃ H ₄	C ₃ H ₆	C ₃ H ₈
$q_{A,sat}$ (mol kg ⁻¹)	2.1	2	2.3
b_A (Pa ^{-ViA})	4.2×10 ⁻²⁷	3.45×10 ⁻⁵⁹	7.87×10 ⁻²⁷
v_A (dimensionless)	8.55	17.5	7.6
$q_{B,sat}$ (mol kg ⁻¹)	0.85	0.7	0.33
b_B (Pa ^{-ViB})	8.16×10 ⁻⁹	1.04×10 ⁻⁶	6.87×10 ⁻¹⁵
v_B (dimensionless)	2.2	1.6	3.6
$q_{C,sat}$ (mol kg ⁻¹)	1.5	0.93	0.49
b_C (Pa ^{-ViC})	4.96×10 ⁻⁵	5.53×10 ⁻⁶	1.1×10 ⁻¹³
v_C (dimensionless)	0.89	1.06	2.8

Table 5 3-site Langmuir-Freundlich parameters for C₃H₄, C₃H₆ and C₃H₈ at 298 K in [Cu(dhbc)₂(4,4'-bipy)].

	C ₃ H ₄	C ₃ H ₆	C ₃ H ₈
$q_{A,sat}$ (mol kg ⁻¹)	0.2	1.63	1.33
b_A (Pa ^{-ViA})	9.72×10 ⁻⁷²	3.5×10 ⁻⁴¹	2.95×10 ⁻⁴⁰
v_A (dimensionless)	18.1	10.5	10.5
$q_{B,sat}$ (mol kg ⁻¹)	1.8	0.94	0.98
b_B (Pa ^{-ViB})	2.91×10 ⁻⁵	1.51×10 ⁻⁵	2.63×10 ⁻⁸
v_B (dimensionless)	0.91	1.07	1.77
$q_{C,sat}$ (mol kg ⁻¹)	1.9	0.6	0.5
b_C (Pa ^{-ViC})	3.38×10 ⁻³⁹	3.26×10 ⁻¹⁰	3.27×10 ⁻¹⁰
v_C (dimensionless)	10.4	0.64	0.65

Notation

b_A Langmuir-Freundlich constant for species i at adsorption site A, Pa^{-ViA}

b_B Langmuir-Freundlich constant for species i at adsorption site B, Pa^{-ViB}

b_C Langmuir-Freundlich constant for species i at adsorption site C, Pa^{-ViC}

E energy parameter, J mol⁻¹

- p_i partial pressure of species i in mixture, Pa
 p_t total system pressure, Pa
 q_i component molar loading of species i , mol kg⁻¹
 q_{st} isosteric heat of adsorption, J mol⁻¹
 t time, s
 T absolute temperature, K

Greek letters

- ν Freundlich exponent, dimensionless

3. Molar enthalpy of gate opening

The Clausius–Clapeyron equation can be used to calculate the molar enthalpy of gate opening, ΔH_{GO} , from the $p_{GO}(T)$ behavior of the adsorption branch of the unary isotherms of C₂H₂, C₂H₄, C₂H₆, C₃H₄, C₃H₆, and C₃H₈ at 273 K, and 298 K using

$$\Delta H_{GO} = RT^2 \left(\frac{\partial \ln p_{GO}}{\partial T} \right) \quad (5)$$

The molar enthalpy of gate opening, ΔH_{GO} , correlates with the molar enthalpy of vaporization,

ΔH_{vap} .

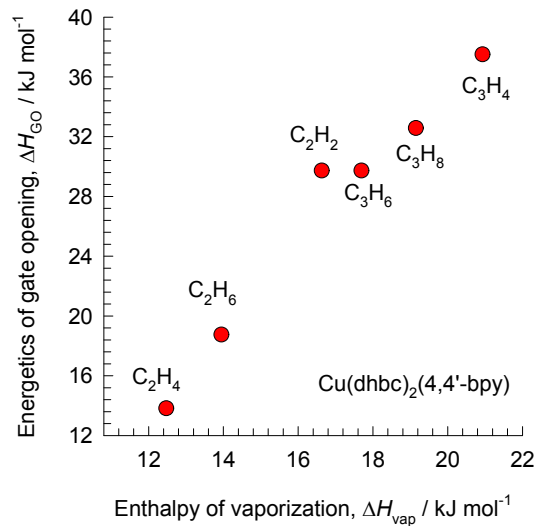


Figure S2. The molar enthalpy of gate opening, ΔH_{GO} , of C₂H₂, C₂H₄, C₂H₆, C₃H₄, C₃H₆, and C₃H₈ at 273 K, and 298 K in [Cu(dhbc)₂(4,4'-bipy)] plotted as a function of latent heats of vaporization.

4. Isotheric heat of adsorption

The isotheric heat of adsorption, Q_{st} , defined as

$$Q_{st} = RT^2 \left(\frac{\partial \ln p}{\partial T} \right)_q \quad (6)$$

were determined using the pure component isotherm fits using the Clausius-Clapeyron equation.

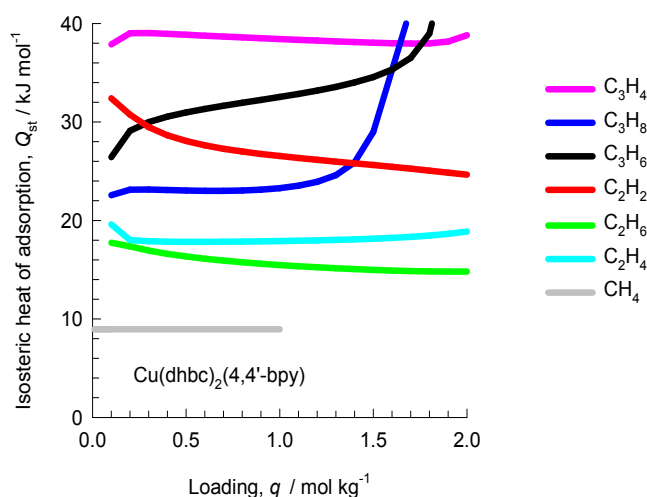


Figure S3. Comparison of the isotheric heat of adsorption of C1-C3 hydrocarbons in [Cu(dhbc)₂(4,4'-bipy)].

5. Grand canonical Monte Carlo (GCMC) simulations

Force fields and Simulation details

The potential parameters and partial charges for all of the adsorbates are shown in Table 6. C₂H₆ and C₂H₄ were modeled as a linear molecule with two charged LJ interaction sites, with C–C bond length $l = 1.54 \text{ \AA}$ and 1.33 \AA , respectively, taken from the EPM2 force field developed by Harris and Yung.¹

Table 6 LJ potential and coulombic potential parameters for the adsorbates.

Adsorbate	Site	LJ parameters		
		$\sigma(\text{\AA})$	$\epsilon/k_b(\text{K})$	charge (e)
C ₂ H ₆	C_C	3.76	108.0	0.0
C ₂ H ₄	C_C	3.96	56.0	0.0

The MOF material studied here was modeled by the atomistic representation. The LJ potential parameters for the framework atoms of the MOFs were taken from the Dreiding force field,² and

the missing parameters for Cu were taken from the universal force field (UFF),³ as given in Table 7. The Lorentz–Berthelot mixing rules were used to determine all of the LJ cross-potential parameters of adsorbate–adsorbate and adsorbate–MOF interactions. In this work, atomic partial charges for the frameworks of the MOFs were estimated using the CBAC method developed by Zhong’s group, with slight variation to make the total charge equal to zero.^{4,5}

Table 7 LJ Potential Parameters for the Atoms in the Framework.

LJ parameters	Cu ^a	C	O	H	N
$\sigma(\text{\AA})$	3.11	3.47	3.03	2.85	3.26
ϵ/k_B (K)	2.516	47.86	48.16	7.65	38.95

^a Taken from the UFF force field (it is missed in the Dreiding force field).

References

1. J. J. Potoff, J. I. Siepmann, *AICHE J.* **2001**, *47*, 1676-1682.
2. S. L. Mayo, B. D. Olafson, W. A. Goddard, *J. Phys. Chem.* **1990**, *94*, 8897-8909.
3. A. K. Rappe, C. J. Casewit, K. S. Colwell, W. A. Goddard, W. M. Skiff, *J. Am. Chem. Soc.* **1992**, *114*, 10024-10035.
4. Q. Xu, C. Zhong, *J. Phys. Chem. C.* **2010**, *114*, 5035-5042.
5. C. Zheng, C. Zhong, *J. Phys. Chem. C.* **2010**, *114*, 9945-9951.

6. MD (Molecule Dynamic) simulations

MD simulations in the *NVT*-ensemble were performed to show gas separation behavior of the membranes by the Forcite module on the basis of the force field of condensed-phase optimized molecular potential for atomistic simulation studies (COMPASS).¹ The temperature was maintained at 273 K using the Andersen thermostat method. A combination of site–site Lennard–Jones (LJ) and Coulombic potentials was employed to determine the intermolecular interactions between adsorbates and adsorbates, as well as between adsorbates and MOF structures.²⁻⁴ During the simulations, the MOFs structure was kept rigid, and C₂H₆ molecules were uniform distributed in the channels constitute an equilibrium system (Fig. 1A). Before MD simulations, the C₂H₆ molecules in one channel were labeled purple and first molecule was labeled yellow as shown in Figure 1 B and C.

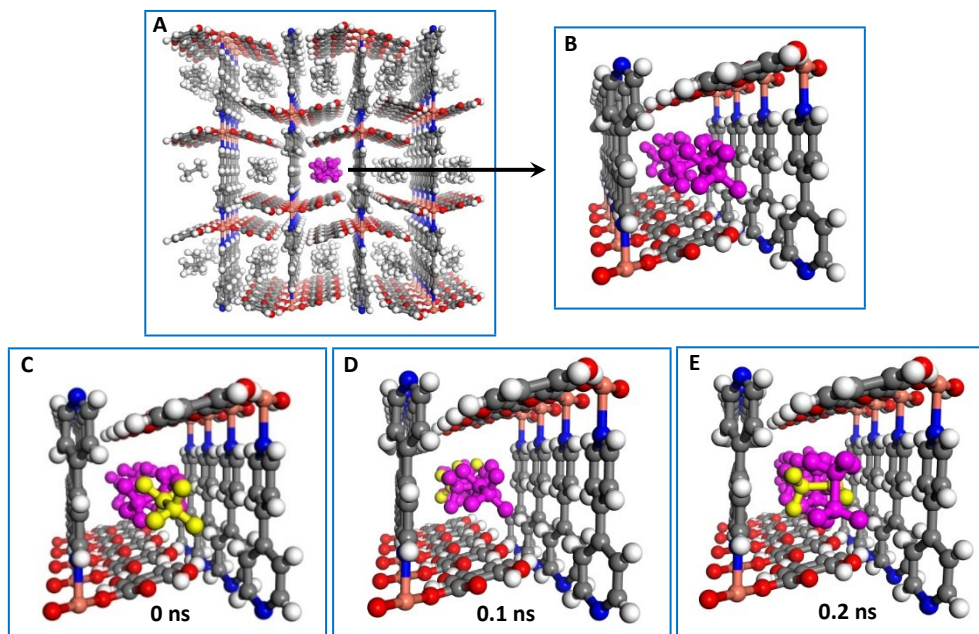


Figure S4. MD simulation for C_2H_6 molecules diffusion in the channels of $[Cu(dhbc)_2(4,4'-bipy)]$ at 1 bar and 273 K.

After the MD simulation time of 0.2 ns, we can see that the labeled C_2H_6 molecular (yellow) can distributed randomly during the entire simulation. It indicated that C_2H_6 molecules can easily diffusion through the one-dimensional channels, and no pore size limitation to diffusion were found.

References

1. Q. Zheng, Y. Geng, S. Wang, Z. Li and J.-K. Kim, *Carbon*, **2010**, 48, 4315.
2. T. Wu, Q. Xue, C. Ling, M. Shan, Z. Liu, Y. Tao and X. Li, *J. Phys. Chem. C*, 2014, **118**, 7369.
3. Y. Tao, Q. Xue, Z. Liu, M. Shan, C. Ling, T. Wu and X. Li, *Acs Appl. Mater. Interfaces*, 2014, **6**, 8048.
4. M. Shan, Q. Xue, N. Jing, C. Ling, T. Zhang, Z. Yan and J. Zheng, *Nanoscale*, 2012, **4**, 5477.

7. IAST calculations of mixture adsorption

Briefly, the basic equation of the Ideal Adsorbed Solution Theory (IAST) theory of Myers and Prausnitz is the analogue of Raoult's law for vapor-liquid equilibrium, i.e.

$$f_i = P_i^0 x_i; \quad i = 1, 2, \dots, n \quad (7)$$

where x_i is the mole fraction in the adsorbed phase

$$x_i = \frac{q_i}{q_1 + q_2 + \dots + q_n} \quad (8)$$

and P_i^0 is the pressure for sorption of every component i , which yields the same spreading pressure, π for each of the pure components, as that for the mixture:

$$\frac{\pi A}{RT} = \int_0^{P_1^0} \frac{q_1^0(f)}{f} df = \int_0^{P_2^0} \frac{q_2^0(f)}{f} df = \int_0^{P_3^0} \frac{q_3^0(f)}{f} df = \dots \quad (9)$$

where R is the gas constant ($= 8.314 \text{ J mol}^{-1} \text{ K}^{-1}$), and $q_i^0(f)$ is the *pure* component adsorption isotherm given by the Langmuir-Freundlich fits. The molar loadings $q_i^0(f)$ are expressed in the units of moles adsorbed per kg of framework, i.e. mol kg^{-1} . The units of the spreading pressure π is the same as that for surface tension, i.e. N m^{-1} . The quantity A on the left side of Equation (9) is the surface area per kg of framework, with units of $\text{m}^2 \text{ kg}^{-1}$.

Each of the integrals in Equation (9) can be evaluated analytically. For the 3-site Langmuir-Freundlich isotherm, the integration yields

$$\int_{f=0}^P \frac{q^0(f)}{f} df = \frac{q_{A,sat}}{v_A} \ln(1 + b_A P^{v_A}) + \frac{q_{B,sat}}{v_B} \ln(1 + b_B P^{v_B}) + \frac{q_{C,sat}}{v_C} \ln(1 + b_C P^{v_C}) \quad (10)$$

The right hand side of equation (10) is a function of P . For multicomponent mixture adsorption, each of the equalities on the right hand side of Equation (9) must be satisfied. These constraints may be solved using a suitable root-finder, to yield the set of values of $P_1^0, P_2^0, P_3^0, \dots, P_n^0$, all of which satisfy Equation (9). The corresponding values of the integrals using these as upper limits of

integration must yield the same value of $\frac{\pi A}{RT}$ for each component; this ensures that the obtained solution is the correct one.

The adsorbed phase mole fractions x_i are then determined from

$$x_i = \frac{f_i}{P_i^0}; \quad i = 1, 2, \dots, n \quad (11)$$

The total amount adsorbed is calculated from

$$q_t \equiv q_1 + q_2 + \dots + q_n = \frac{1}{\frac{x_1}{q_1^0(P_1^0)} + \frac{x_2}{q_2^0(P_2^0)} + \dots + \frac{x_n}{q_n^0(P_n^0)}} \quad (12)$$

The set of equations (7), (8), (9) (10), and (12) need to be solved numerically to obtain the loadings, q_i of the individual components in the mixture.

The selectivity of preferential adsorption of component i over component j can be defined as

$$S_{ads} = \frac{q_i/q_j}{p_i/p_j} \quad (13)$$

In equation (13), q_i and q_j are the *absolute* component loadings of the adsorbed phase in the mixture.

8. Transient breakthroughs in fixed bed adsorber

The performance of industrial fixed bed adsorbers is dictated by a combination of adsorption selectivity and uptake capacity. To demonstrate the selective adsorption of propyne using $\text{Cu}(\text{dhbc})_2(4,4'\text{-bpy})$ we perform transient breakthrough simulations using the simulation methodology described in earlier work.

A brief summary of the breakthrough simulation methodology, essentially the same as that presented by Krishna, is provided below.

Assuming plug flow of an n -component gas mixture through a fixed bed maintained under isothermal conditions, the partial pressures in the gas phase at any position and instant of time are obtained by solving the following set of partial differential equations for each of the species i in the gas mixture.

$$\frac{1}{RT} \frac{\partial p_i(t, z)}{\partial t} = -\frac{1}{RT} \frac{\partial (v(t, z)p_i(t, z))}{\partial z} - \frac{(1-\varepsilon)}{\varepsilon} \rho \frac{\partial \bar{q}_i(t, z)}{\partial t}; \quad i = 1, 2, \dots, n \quad (13)$$

In equation (13), t is the time, z is the distance along the adsorber, ρ is the framework density, ε is the bed voidage, v is the interstitial gas velocity, and $\bar{q}_i(t, z)$ is the *spatially averaged* molar loading within the crystallites of radius r_c , monitored at position z , and at time t .

At any time t , during the transient approach to thermodynamic equilibrium, the spatially averaged molar loading within the crystallite r_c is obtained by integration of the radial loading profile

$$\bar{q}_i(t) = \frac{3}{r_c^3} \int_0^{r_c} q_i(r, t) r^2 dr \quad (14)$$

For the breakthrough simulations presented in this article, we assume that intra-crystalline diffusion is of negligible importance. With this assumption the entire crystallite particle can be considered to be in thermodynamic equilibrium with the surrounding bulk gas phase at that time t ,

and position z of the adsorber

$$\bar{q}_i(t, z) = q_i(t, z) \quad (15)$$

The molar loadings at any position z , at time t in Equation (15) are calculated on the basis of adsorption equilibrium with the bulk gas phase partial pressures p_i at that position z and time t . The adsorption equilibrium can be calculated on the basis of the Ideal Adsorbed Solution Theory (IAST) of Myers and Prausnitz. In all the simulation results we present in this article, the IAST calculations use Langmuir-Freundlich isotherm fits.

The *interstitial* gas velocity is related to the *superficial* gas velocity by

$$v = \frac{u}{\varepsilon} \quad (16)$$

In industrial practice, the most common operation is with to use a step-wise input of mixtures to be separation into an adsorber bed that is initially free of adsorbates, i.e. we have the initial condition

$$t = 0; \quad q_i(0, z) = 0 \quad (17)$$

At time, $t = 0$, the inlet to the adsorber, $z = 0$, is subjected to a step input of the n -component gas mixture and this step input is maintained till the end of the adsorption cycle when steady-state conditions are reached.

$$t \geq 0; \quad p_i(0, t) = p_{i0}; \quad u(0, t) = u \quad (18)$$

where u is the superficial gas velocity at the inlet to the adsorber. The model parameters are chosen on the basis of the experimental set-up and operating conditions.

9. Measurement of breakthrough experiment

The pelleting process of [Cu(dhbc)₂(4,4'-bipy)] particles were reported in our previous work.¹ In the separation experiment, [Cu(dhbc)₂(4,4'-bipy)] (4.1380 g) particles with diameters of 200-300 μm were prepared and packed into φ9×150 mm stainless steel column. The experimental set-up consisted of two fixed-bed stainless steel reactors. One reactor was loaded with the adsorbent, while the other reactor was used as a blank control group to stabilize the gas flow. The horizontal reactors were placed in a temperature controlled environment, maintained at 298 or 273 K. The

flow rates of all gases mixtures were regulated by mass flow controllers, an air cushion tank was placed to keep the gases mixtures well-mixed, and the effluent gas stream from the column is monitored by a gas chromatography. Prior to the breakthrough experiment, we activated the sample by flushing the adsorption bed with helium gas for 2 h at 373 K. Subsequently, the reactor was allowed to equilibrate at the measurement rate before we switched the gas flow.

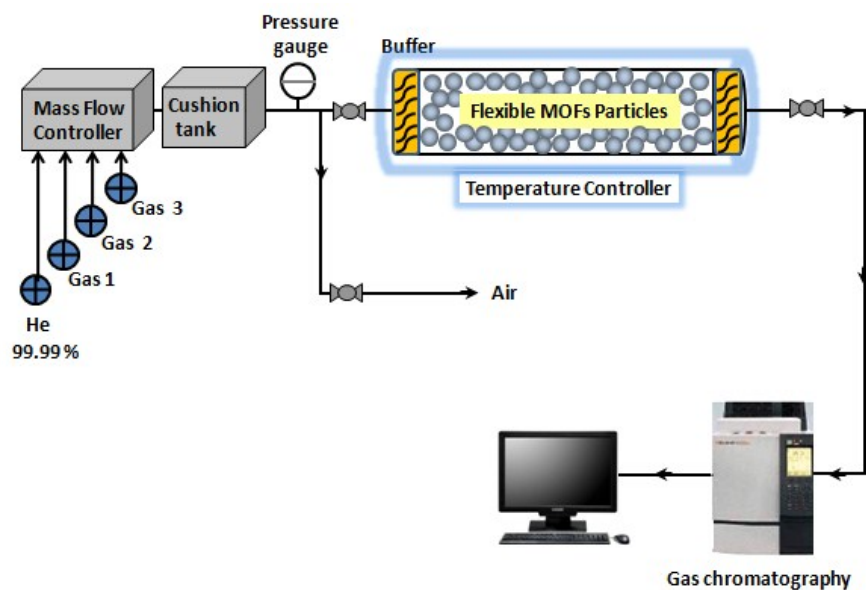


Figure S5. Breakthrough separation apparatus for flexible MOFs.

10. C_2H_2 - C_2H_4 - C_2H_6 separation

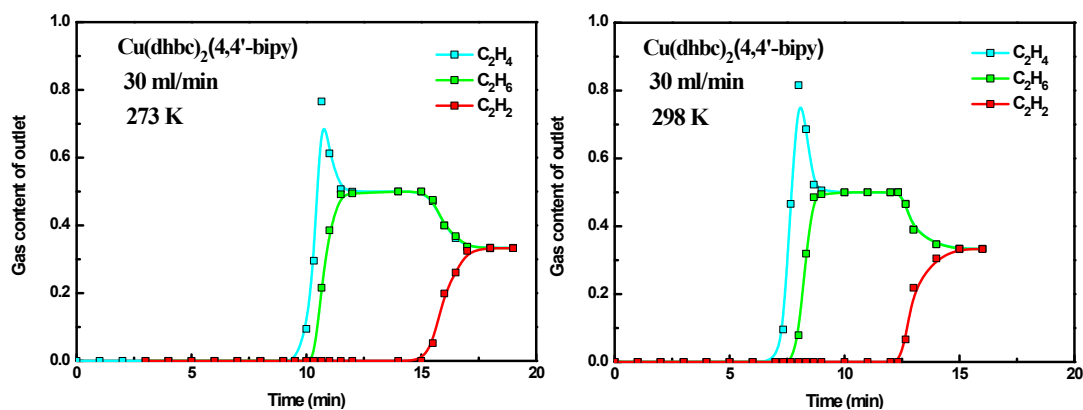


Figure S6. Breakthrough curves of [Cu(dhbc)₂(4,4'-bipy)] for separation equimolar 3-component C₂H₆-C₂H₄-C₂H₂ mixture in a fixed bed of adsorbent at flow rates of 30 ml/min at 1 bar and 273 and 298 K.

11. CH₄-C₂H₆-C₃H₈ separation

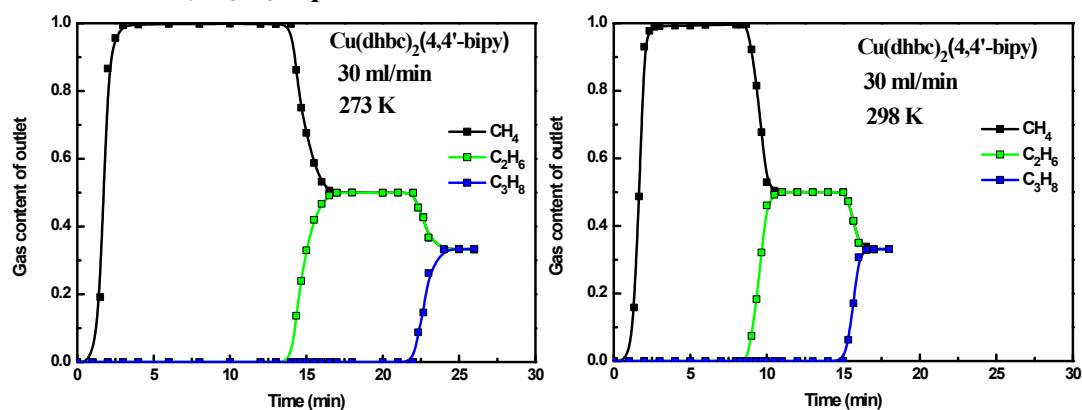


Figure S7. Breakthrough curves of [Cu(dhbc)₂(4,4'-bipy)] for separation equimolar 3-component CH₄-C₂H₆-C₃H₈ mixture in a fixed bed of adsorbent at flow rates of 30 ml/min at 1 bar and 273 and 298 K.

12. C₂H₄-C₃H₆ separation

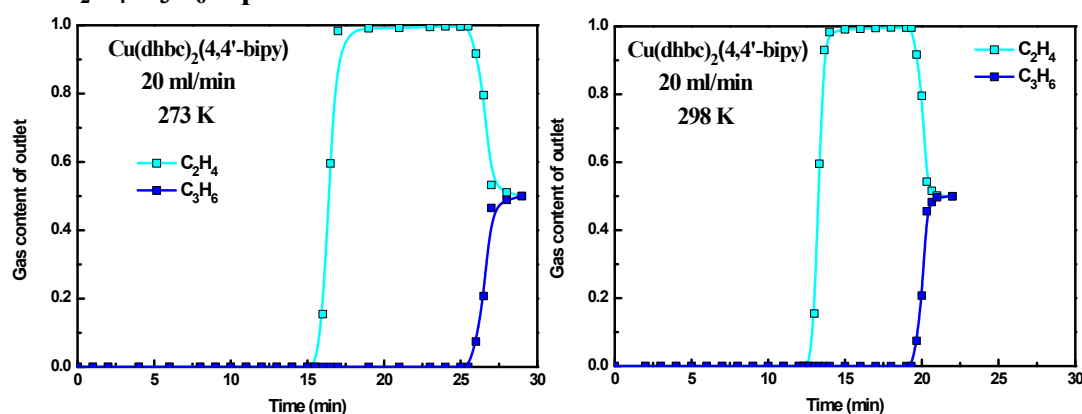


Figure S8. Breakthrough curves of [Cu(dhbc)₂(4,4'-bipy)] for separation equimolar C₂H₄-C₃H₆ mixture in a fixed bed of adsorbent at flow rates of 20 ml/min at 1 bar and 273 and 298 K.